arXiv:0809.1215v2 [cond-mat.supr-con] 21 Jan 2009

Voltage-current and voltage-flux characteristics of asymmetric high T_C DC SQUIDs.

I. L. Novikov,[1] Ya. S. Greenberg,[1] V. Schultze,[2] R. IJsselsteijn,[2] and H.-G. Meyer[2]

[1]*Novosibirsk State Technical University, 20 K. Marx Ave., 630092 Novosibirsk, Russia.*
[2]*Institute of Photonic Technology, Jena, Germany*

(Dated: January 21, 2009)

We report measurements of transfer functions and flux shifts of 20 on-chip high T_C DC SQUIDs half of which were made purposely geometrically asymmetric. All of these SQUIDs were fabricated using standard high T_C thin film technology and they were single layer ones, having 140 nm thickness of $YBa_2Cu_3O_{7-x}$ film deposited by laser ablation onto MgO bicrystal substrates with 24^0 misorientation angle. For every SQUID the parameters of its intrinsic asymmetry, i. e., the density of critical current and resistivity of every junction, were measured directly and independently. We showed that the main reason for the on-chip spreading of SQUIDs' voltage-current and voltage-flux characteristics was the intrinsic asymmetry. We found that for SQUIDs with a relative large inductance ($L > 120$ pH) both the voltage modulation and the transfer function were not very sensitive to the junctions asymmetry, whereas SQUIDs with smaller inductance ($L \simeq 65 - 75$ pH) were more sensitive. The results obtained in the paper are important for the implementation in the sensitive instruments based on high T_C SQUID arrays and gratings.

PACS numbers: 74.50.+r

I. INTRODUCTION

The high-transition-temperature superconducting quantum interference devices (high-T_C DC SQUIDs) each consisting of two bicrystal Josephson junctions are key elements for many sensitive instruments such as extremely low noise magnetometers[1,2,3], the series- and parallel- SQUID arrays[4,5], the superconducting quantum interference grating[6,7], etc.

However, the further developments of these devices are limited by significant on chip spreading in the critical current and normal resistance of high T_C Josephson junctions which seems to be unavoidable for grain-boundary junctions.[8,9,10,11,12].

The different values of critical current and normal resistance of two Josephson junctions result in turn in the vast spreading of the output voltage-current (VCC) and voltage flux (VFC) characteristics for on chip high T_C DC SQUIDs[13,14,15].

The influence of the junction asymmetry on the output characteristics of high T_C DC SQUIDs has been analyzed in[16,17,18,19,20], where it was shown that the transfer function for asymmetric SQUIDs can be substantially differ from that of symmetric SQUIDs.

The extensive comparison of experimental characteristics of intentionally fabricated asymmetric high T_C DC SQUID with computer simulations has been performed in[17], where in most cases a reduction of the voltage-to-flux transfer function of the asymmetric SQUID as compared to the symmetric SQUID has been observed.

From the other point the output characteristics of high T_C DC SQUIDs can be used to infer the information about the on chip distribution of the critical currents and normal resistances of the Josephson junctions[11,12].

In known experiments[11,12,17] the asymmetry of critical current of two Josephson junctions in DC SQUID loop has been determined indirectly from the measured flux shift of the voltage-flux curve. Since for high T_C Josephson junctions the density of critical current and the resistivity of the junction are interrelated, it also influences the value of the last quantity. In addition, as is shown in the paper, this method has a restricted range of validity. That is why, as was noted in[17], a clear-cut comparison between simulation and experimental data requires the independent experimental determination of the current and resistance asymmetry.

Therefore, the main purpose of our paper is the independent and direct determination of the current and resistance asymmetry and the investigation of the influence of the junctions asymmetry on the scattering over the chip of the main output parameters of DC SQUID, i.e., its voltage modulation, voltage-to-flux transfer function, flux shift.

To this end we investigated 20 purposely made asymmetric high T_C DC SQUIDs. For the first time we measured independently and directly the current and resistance asymmetry for every junction in the interferometer loop. We show that the main reason for the junctions asymmetry is the on-chip spreading in the resistivity and the critical current density. Even for a geometrically symmetric design of the interferometer the critical current densities of the two junctions may be substantially different. We found that, in general, both the voltage modulation and the transfer function are not very sensitive to the junctions asymmetry, whereas the flux shift of the VFC shows approximately linear dependance on asymmetry parameters.

The paper is organized as follows. In Section II the current and resistance asymmetry for the junctions of DC SQUID are defined and the analytical expressions for transfer function and flux shift for asymmetric DC SQUID are given. The experimental part of the paper is in detail described in Section III. Section IV is devoted to an extensive analysis of the influence of SQUID asym-

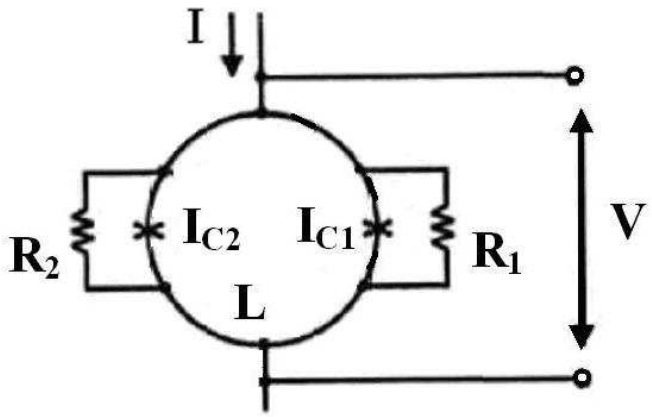

FIG. 1: The asymmetric DC SQUID

metry on the transfer function and flux shift of VFC. Obtained results are shortly summarized in Section V.

II. ASYMMETRIC DC SQUID

A. The asymmetry parameters

An asymmetric DC SQUID shown in Fig.1 consists of a superconducting loop of inductance L intersected by two Josephson junctions, which have different critical currents I_{C1}, I_{C2} and normal resistances R_1, R_2. The capacitances of the two junctions, which are not shown in Fig.1 are assumed to be equal. In order to describe the junctions asymmetry we define the average values of the critical current I_C and resistance R, and a current asymmetry γ and a resistance asymmetry ρ as follows: $I_{C1} = (1+\gamma)I_C$, $I_{C2} = (1-\gamma)I_C$, $R_1 = R/(1+\rho)$, $R_2 = R/(1-\rho)$, where

$$I_C = \frac{I_{C1}+I_{C2}}{2} \equiv \frac{I_{SQ}}{2}, \;\; \gamma = \frac{I_{C1}-I_{C2}}{I_{C1}+I_{C2}} \qquad (1)$$

$$R = \frac{2R_1R_2}{R_1+R_2} \equiv 2R_{SQ}, \;\; \rho = \frac{R_2-R_1}{R_1+R_2} \qquad (2)$$

Note that the SQUID critical current I_{SQ} and its resistance R_{SQ} are being measured directly from the voltage-current characteristic of the DC SQUID.

There are two different origins of the junction asymmetry: geometrical asymmetry and intrinsic asymmetry[17]. For bicrystal grain boundary junctions geometric asymmetry is associated with the different width w of the junctions. We describe geometric asymmetry by the parameter α_g according to $w_1 = (1+\alpha_g)w$ and $w_2 = (1-\alpha_g)w$, with $w = (w_1+w_2)/2$. The intrinsic asymmetry is associated with different values of the current density j_0 and the resistivity ρ_0 for two junctions. We describe intrinsic asymmetry by the parameters α_j and α_ρ according to[17]:

$$j_{01} = j_0(1+\alpha_j), \;\; \rho_1 = \rho_0/(1+\alpha_\rho)$$
$$j_{02} = j_0(1-\alpha_j), \;\; \rho_2 = \rho_0/(1-\alpha_\rho) \qquad (3)$$

The parameters of intrinsic asymmetry α_j and α_ρ can be obtained from the independent measurements of the parameters of the bulk asymmetry γ, ρ and geometric asymmetry α_g[17]:

$$\alpha_j = \frac{\gamma-\alpha_g}{1-\alpha_g\gamma}, \;\; \alpha_\rho = \frac{\rho-\alpha_g}{1-\alpha_g\rho} \qquad (4)$$

Since high T_C Josephson junctions obey the scaling law $I_CR \approx j_c^{1/2}$[21], the parameters α_j and α_ρ are interrelated to each other[17]

$$\alpha_\rho = \frac{1-\sqrt{1-\alpha_j^2}}{\alpha_j}, \;\; \alpha_j = \frac{2\alpha_\rho}{1+\alpha_\rho^2} \qquad (5)$$

B. Output voltage across asymmetric SQUID

In general, the output voltage across asymmetric SQUID is the complicated function of several dimensionless parameters[20]: $V = F(i, \alpha, \beta, \Gamma, \varphi_X, \rho, \gamma)$, where $i = I/I_C$ (I is the bias current); $\alpha = L/L_F$ ($L_F = (\Phi_0/2\pi)^2/k_BT$ is the fluctuation inductance which is equal approximately to 100 pH at T=77 K); $\beta = 2LI_C/\Phi_0$; $\Gamma = 2\pi k_BT/\Phi_0I_C$ is the noise parameter (k_B is Boltzmann constant, T is absolute temperature); $\varphi_X = \pi\Phi_X/\Phi_0$ (Φ_X is the external magnetic flux, Φ_0 is the flux quantum). Three parameters α, β, Γ are not independent, but are subject to the relation $\alpha = \pi\beta\Gamma$.

There are several properties of the output characteristics of asymmetric SQUIDs which allow one to identify them by experiment[20]. First, in the presence of applied flux the voltage across asymmetric SQUIDs is not an odd function of the bias current, i. e., $V(-i) \neq -V(i)$. Thus, the quantity $V(-i)+V(i)$ can be used as one of the measure of SQUID asymmetry. It is a periodic function of the applied flux and it depends on the bias current and on the parameters of asymmetry.

The second property which is known for a long time (see, for example, Ref.22) is the shift of the voltage-flux characteristic (VFC) under reversal of the bias current. The shift is commonly attributed to the asymmetry in the critical current of the two junctions:

$$\Delta\Phi = L(I_{C1}-I_{C2}) = \gamma\beta\Phi_0 \qquad (6)$$

This property has been widely used for experimental determination of the current asymmetry[11,12,17,23]. However, the expression (6) cannot describe some experimental facts. In particular, it does not depend on the bias current while the experimental flux shift does depend on i. For large inductance DC SQUIDs the picture is more complicated[20]. There is no simple relation between current asymmetry and a flux shift. In addition, asymmetry

in resistance contributes also to the total flux shift. The expression for the flux shift under a reversal of the bias current is as follows[20]:

$$\frac{\Delta\Phi_X}{\Phi_0} = \frac{1}{\pi}\Theta(i,\Gamma,\rho,\gamma) + \frac{\rho\alpha}{2\pi\Gamma}i \qquad (7)$$

The explicit expression for the quantity Θ which is too cumbersome one can find in Ref. 20 (Eq. 31b).

As is seen from (7) the flux shift is a complicated function of the bias current and the parameters of asymmetry. The dependance on SQUID inductance L is hidden in the second term in (7). Due to the relation $\alpha = \pi\beta\Gamma$ this term can be written as $\rho i\beta/2$, which is equivalent to the expression found for the flux shift in the limit of a large bias current i[24].

It is worth noting that for $i > 0$ the voltage-flux curve is shifted to the negative side of the flux ($\Delta\Phi_X < 0$) relative to a symmetric voltage-flux curve, while for the reversed bias ($i < 0$) the voltage-flux curve is shifted to the positive side of the flux ($\Delta\Phi_X > 0$).

C. Transfer function of asymmetric SQUID

As is known, the shape of experimental VFC is not symmetric. The asymmetry of the junctions induces distortion of the $V(\Phi)$-curves, which leads to different values of V_Φ^+ and V_Φ^- for the maximum positive and negative slope of the $V(\Phi)$-curves, respectively. The impact of the asymmetry on the transfer function has been studied by computer simulations in Ref. 17. It was shown that the normalized transfer function $v_\Phi^\pm = V_\Phi^\pm\Phi_0/RI_C$ can be factorized as $v_\Phi^\pm = g^\pm(\Gamma\beta)f^\pm(\gamma,\beta)$. The explicit analytical expressions for the quantities $g^+(\Gamma\beta)$ and $f^+(\gamma,\beta)$ for limited range of parameters Γ and β ($\Gamma\beta < 1$, $\beta < 5$) have been given in Ref. 17.

III. EXPERIMENTAL

1. *High-T_C DC SQUID preparation and characterization*

The principal layout of an asymmetric high-T_C DC SQUID is shown in Fig. 2. It consists of the interferometer loop and two Josephson junctions with different widths. A total of 20 such SQUIDs was integrated on one chip. All have the same superconducting loop width of 8 μm and slit width of 4 μm, respectively. Three different slit lengths of 25 μm, 75 μm and 125 μm were used, what partitions the SQUIDs into three groups: small (S SQUID), medium (M SQUID) and large ones (L SQUID). The slit lengths are reflected in SQUID inductance ranges of L∼65-75 pH, L∼125-135 pH and L∼185-195 pH for the S, M and L SQUIDs, respectively. Within the groups, parameters of asymmetry were varied, using various junction widths w_1 and w_2 between 0.4 and 1.2 μm. All SQUIDs were connected via a common superconducting

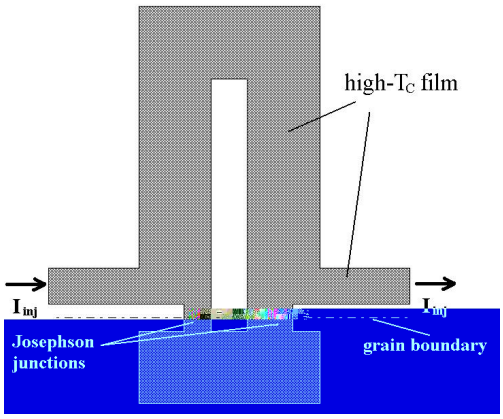

FIG. 2: Design of asymmetric high-T_C DC SQUID

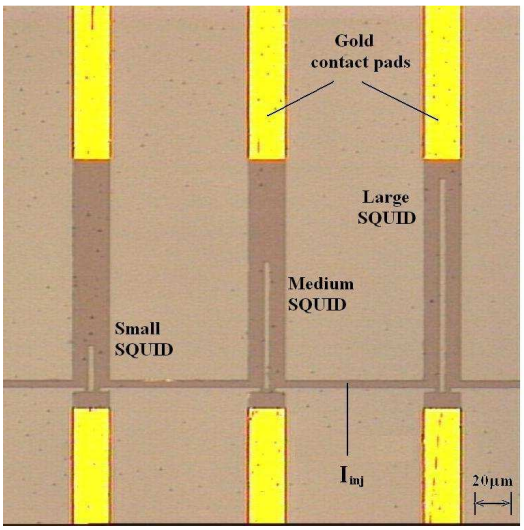

FIG. 3: Color online. Photography of three asymmetric high-Tc DC SQUIDs.

line, which was used to inject a DC current I_{inj} into the SQUIDs. Figure 3 shows a photograph of three SQUIDs connected that way.

The SQUIDs were fabricated using a standard thin-film technology, which was described in detail in Ref. 25. Using laser ablation, a 140 nm thick YBCO film is deposited onto a 24^0 MgO bicrystal substrate with 10 mm x 10 mm x 1 mm dimension. On top of the non-structured YBCO film a 100 nm thick gold layer was deposited by thermal evaporation and subsequently structured by lift-off. Finally, the YBCO layer was patterned using standard e-beam lithography and ion-beam-etching. As already shown in[25], Josephson junctions with widths down to 0.4 μm show no degradation in critical current density. In addition, the chip was covered by a Teflon layer which protected it from water during thermo cycling[26]. Then the SQUID chip was glued on a non-metallic holder

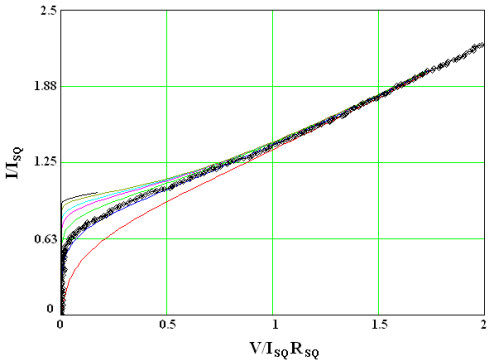

FIG. 4: Color online. Determination of critical current from experimental VCC (thick line). The critical current I_C to which the experimental VCC is normalized, is varied until the normalized experimental VCC fits to one of the theoretical VCCs (thin lines).

with a wire-wound coil beneath, which was used to apply magnetic flux to the SQUIDs.

All measurements were performed in liquid nitrogen at 77 K in a well shielded environment. First, for every SQUID we have measured its voltage-current (VCC) and voltage-flux (VFC) characteristics. Second, one of the two junctions in the loop was measured directly. For that after all the measurements at the SQUIDs have been performed, all SQUID loops have been cut to allow the independent measurements of the characteristics of one junction per SQUID. To do that the right superconducting arm of every SQUID loop was removed by additional optical lithography and chemical etching. This allowed to measure the critical current and normal resistance of the Josephson junction in the remaining arm of the SQUID. Therefore, we determined for the first time independently and directly the current density and resistivity for every junction in the interferometer loop which allowed us to investigate their influence on the SQUID characteristics.

2. *SQUID characteristics*

The first group of measurements concerned the characterization and classification of the SQUIDs. All these parameters are listed in Table I.

Within the groups (S, M, L) the junction sizes w_1 and w_2 are varied between 0.4 and 1.2 μm, yielding the geometrical asymmetry α_g. Here, the junction widths are layout parameters. The resulting SQUID inductance L was actually determined, however. This was done in the following way.

The injection current I_{inj} flows around the upper part of the SQUID loop (see Fig. 2). This coupling part of the SQUID has an inductance of L_c which can be measured, because the injection current produces a magnetic flux Φ_c=L_c I_{inj} in the SQUID loop. The measured voltage-

TABLE I: DC SQUID parameters; w_1, w_2 are junctions' widths; α_g accounts for geometric asymmetry; L, I_{SQ}, R_{SQ} are the DC SQUID inductance, its critical current and normal resistance; ΔV_{max} is the maximum swing of the VFC; I_{max} is the bias current which provides ΔV_{max}.

SQUID#group	w_1,w_2 μm	α_g	L pH	I_{SQ} μA	R_{SQ} Ω	ΔV_{max} μV	I_{max} μA
1 S	0.6, 0.6	0	71.4	36	3.95	35.8	29.5
2 S	0.6, 0.6	0	71.4	22	5.79	48.2	22.1
3 S	0.8, 0.4	0.33	73.8	35	2.99	21.8	35.3
4 S	0.8, 0.8	0	65.4	29.5	4	38.8	25.6
5 S	1, 0.6	0.25	66.6	25.5	4.82	43.8	23.1
6 S	1.2, 0.4	0.5	70.6	42	3.4	35.6	36.1
7 M	0.6, 0.6	0	131.6	31	4.93	21.5	28
8 M	0.6, 0.6	0	131.6	33	3.87	16.4	26.3
9 M	0.8, 0.4	0.33	134.1	40	4.56	16.4	32.1
10 M	0.8, 0.8	0	125.7	30.5	4.11	16.9	25
11 M	0.8, 0.8	0	125.7	56.5	2.61	12.2	51.2
12 M	1, 0.6	0.25	126.8	55	3.1	15.1	45.1
13 M	1, 0.6	0.25	126.8	35	3.27	14.5	29.7
14 M	1.2, 0.4	0.5	130.5	42	3.55	15.5	39.5
15 M	1.2, 0.4	0.5	130.5	53	2.76	13.7	48.3
16 L	0.6, 0.6	0	191.5	29	4.34	9.2	24.2
17 L	0.8, 0.4	0.33	194.1	25.5	4.68	8	19
18 L	0.8, 0.8	0	185.8	46	3.41	6.7	30.4
19 L	1, 0.6	0.25	186.7	35	3.56	8.4	31.5
20 L	1.2, 0.4	0.5	190.9	49	2.87	4.9	41.1

flux characteristics is periodical in Φ_0, what gives the needed assignment between measured flux and injected current. Thus, the coupling inductance can be determined. In the next step, the coupling inductance was calculated with an algorithm described in[27], which takes into account geometrical and kinetic inductance as well. The London penetration depth λ_L of the high-T_c film acts as a fitting parameter to meet the measured coupling inductance. This λ_L could be determined very consistently to (462 $\pm$ 11) nm for all the 20 SQUIDs. Now, using this known London penetration depth, the whole SQUID inductance could be reliably calculated in the same way.

The normal resistance of the SQUIDs, R_{SQ} was determined from the steepness of the resistive part of VCC at large currents (I > 10 I_{SQ}). Now, knowing the normal resistance of the SQUID, its critical current I_{SQ} can be assessed. The direct extraction from the experimental VCC is difficult due to the large level of thermal noise, which gives strong rounding of the curves. To get access to the noise-free intrinsic critical current of the SQUID, a set of theoretical VCCs is calculated, which were obtained from an analytical solution of the SQUID equations in the small inductance limit[28] (see Fig. 4). In comparison to this set of theoretical VCCs (current normalized to I_{SQ} vs. voltage normalized to the $I_{SQ}R_{SQ}$ product) the experimental VCC is plotted. Because R_{SQ} is known, the noise-free critical current I_{SQ} can be tuned

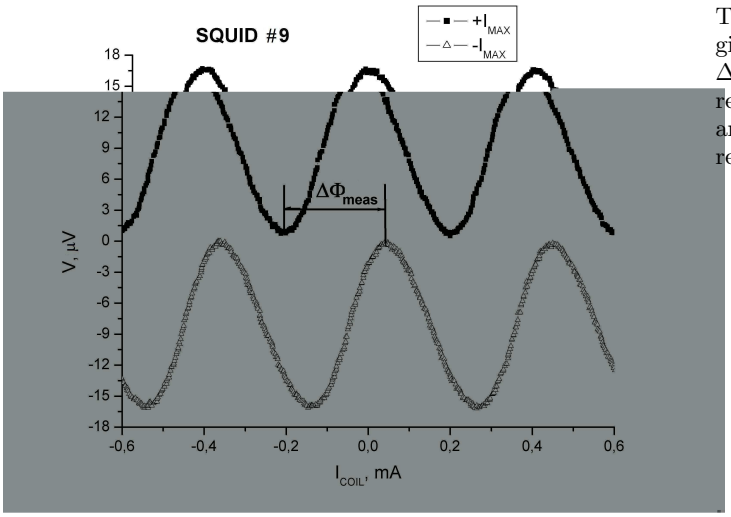

FIG. 5: Experimental VFC for SQUID #9. A measured flux shift $\Delta\Phi_{meas}$ is determined as a distance between the first extremums of VFCs relative to zero flux point ($I_{coil} = 0$).

until the experimental curve fits well to any of the theoretical ones.

The maximum voltage modulation ΔV_{max} and the bias current I_{max} needed for that voltage swing could directly be taken from the measurement of the voltage-flux characteristics.

At the bias current I_{max}, which gave the maximum swing of the VFC (both shown in Table I), the next SQUID parameters were measured. They are presented in Table II. The transfer functions $V_\Phi^\pm$ represents the maximum steepness of VFC at their left (+) and right (-) sides. As VFC is a Φ_0 periodic function, a unique determination of the actual shift $\Delta\Phi_{max}$, which is given in the second column of Table II, is not, in general, possible. Below in Section IVB we describe in detail a reasonable procedure which relates $\Delta\Phi_{max}$ with $\Delta\Phi_{meas}$ defined as the distance between the first extremums of VFCs relative to zero flux ($I_{coil} = 0$, see Fig. 5).

The asymmetry parameters of the SQUIDs are given in Table III.

Unlike the method of Ref. 17, where the asymmetry of the critical current was assessed indirectly from the flux shift of the VFC, we determined the asymmetry parameters by a direct measurement of critical current and resistance of one of the two junctions in the SQUIDs. This got possible due to the opening of one superconducting arm of every SQUID loop.

The first parameters given in Table III, the critical current I_C and resistance R are average junction values for the SQUID as defined in (1), (2). They differ from the SQUID values given in Table I by a factor of 2. For a symmetric SQUID these are just the values of each of the two junctions. The quantities I_2 and R_2 are critical current and resistance of the second junction which remained for the measurement after the SQUID loop had been cut. Using all these data, we obtain the bulk asymmetries γ and ρ using equations (1) and (2), and, finally, with the aid of equations (4), the intrinsic asymmetries α_j and α_ρ. So, for the first time the asymmetry parameters of the current density and resistivity of the junctions in high T_C DC SQUIDs were determined independently and directly.

TABLE II: DC SQUID parameters for the bias current I_{max} given in Table I, where maximum swing ΔV_{max} is provided; $\Delta\Phi_{max}$ is the flux shift of the VFC under reversal of I_{max}; $V_\Phi^\pm$ represents the maximum steepness of the VFC at their left (+) and right (-) sides; $\Delta V_{max}/R$ is the maximum voltage swing related to the average junction resistance (see Table III).

SQUID# group	$\Delta\Phi_{max}$ Φ_0	V_Φ^+ $\mu V/\Phi_0$	V_Φ^- $\mu V/\Phi_0$	$\Delta V_{max}/R$ $\mu V/\Omega$
1 S	0.357	115.7	-99.7	4.531
2 S	0.532	170.1	-147.3	4.163
3 S	0.675	71.3	-60.01	5.234
4 S	0.23	129.5	-116	4.855
5 S	0.412	120.13	-167.3	4.548
6 S	1.243	102.89	-121.4	5.236
7 M	1.36	74.64	-59.97	2.183
8 M	0.079	50.74	-48.11	2.123
9 M	1.656	57.49	-41.19	1.798
10 M	-1.124	52.44	-51.26	2.056
11 M	0.81	36.57	-37.72	2.341
12 M	0.842	45.53	-45.08	2.437
13 M	1.344	49.85	-37.34	2.215
14 M	1.985	52.38	-41.92	2.187
15 M	1.792	41.95	-34.51	2.482
16 L	0.947	22.6	-22.29	1.060
17 L	0.948	22.58	-25.24	0.851
18 L	-0.415	17.74	-20.19	0.979
19 L	1.455	23.96	-23.69	1.181
20 L	2.934	13.49	-15.79	0.850

Before we discuss the influence of junction asymmetry on the output SQUID characteristics we should like to show to what extent our high T_C Josephson junctions obey the scaling law $I_C R \approx j_c^{1/2}$[21]. In this case the parameters α_j and α_ρ are interrelated to each other by Eqs. 5[17]. A theoretical dependance of α_j on α_ρ (second of Eqs. 5) for this scaling law together with experimental points is shown in Fig. 6. As is seen from this figure most of the experimental points are grouped over the theoretical curve. Therefore, we may conclude that our high T_C Josephson junctions are described by the aforementioned scaling law with a good accuracy.

IV. DISCUSSION

A. The depth of the voltage modulation

In general, the increase of the SQUID inductance leads to a decrease of the voltage swing of VFC[1]. This is illus-

TABLE III: Current and resistance asymmetry of DC SQUID.

SQUID# group	I_C μA	R Ω	I_{C2} μA	R_2 Ω	γ	ρ	α_j	α_ρ
1 S	18	7.9	11	9.45	0.39	0.16	-0.39	-0.16
2 S	11	11.58	9	13.56	0.18	0.15	-0.18	-0.15
3 S	17.5	5.98	7.8	12.09	0.55	0.51	-0.269	-0.216
4 S	14.75	7.99	12.5	8.69	0.15	0.08	-0.15	-0.08
5 S	12.75	9.63	8.5	13.05	0.33	0.26	-0.087	-0.011
6 S	21	6.8	12	12.77	0.43	0.47	0.089	0.039
7 M	15.5	9.85	4.2	23.84	0.73	0.59	-0.73	-0.59
8 M	16.5	7.73	15	8.32	0.09	0.07	-0.09	-0.07
9 M	20	9.12	3	18.77	0.85	0.51	-0.723	-0.216
10 M	15.25	8.22	23	5.26	-0.51	-0.56	0.51	0.56
11 M	28.25	5.21	20.5	6.03	0.28	0.14	-0.28	-0.14
12 M	27.5	6.2	24	7.13	0.13	0.13	0.124	0.124
13 M	17.5	6.54	5.9	13.71	0.76	0.52	-0.63	-0.31
14 M	21	7.09	3.6	25.74	0.83	0.72	-0.564	-0.344
15 M	26.5	5.52	9.8	12.43	0.63	0.56	-0.19	-0.083
16 L	14.5	8.68	6.5	13.21	0.55	0.34	-0.55	-0.34
17 L	12.75	9.35	5.3	13.62	0.58	0.31	-0.309	0.022
18 L	23	6.82	28.5	5.58	-0.24	-0.22	0.24	0.22
19 L	17.5	7.11	8.8	11.46	0.5	0.38	-0.286	-0.144
20 L	24.5	5.74	6.4	16.69	0.74	0.66	-0.381	-0.239

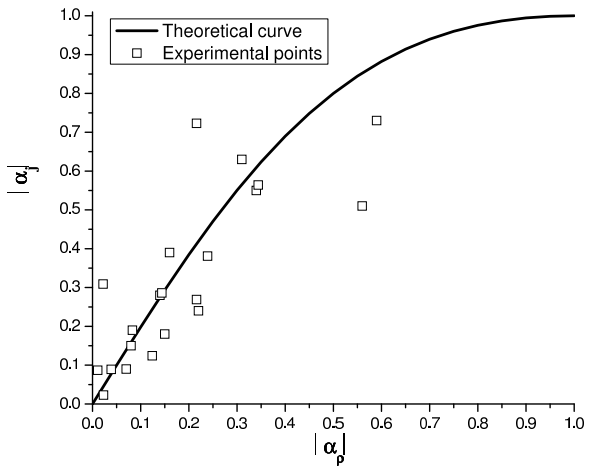

FIG. 6: The dependance of α_j on α_ρ. The theoretical dependance was calculated from the second of Eqs. 5.

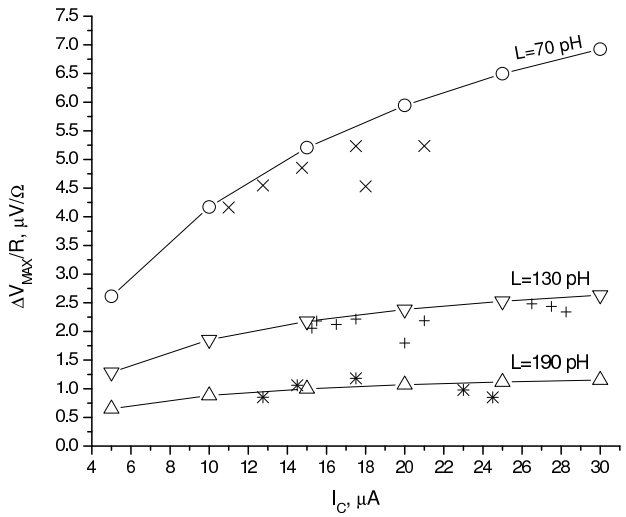

FIG. 7: The voltage modulation as a function of the critical current. The lines for L=70 pH (◯), 130 pH (▽), and 190 pH (△) are calculated from Eq. 8. The experimental points are shown by × for S-SQUIDs, + for M-SQUIDs, and ⋇ for L-SQUIDs.

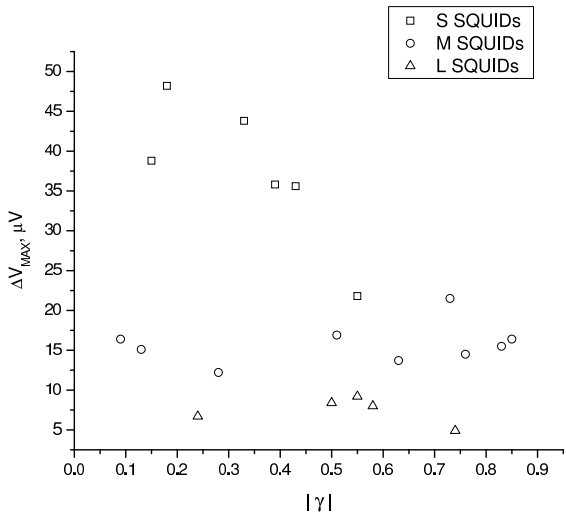

FIG. 8: The depth of the voltage modulation as a function of the critical current asymmetry γ.

trated in Fig. 7 where the voltage modulation $\Delta V_{max}/R$ is shown as a function of the junction critical current. As is seen from the figure the SQUIDs are grouped by their inductance near corresponding lines obtained from the expression of Enpuku[29].

$$\frac{\Delta V}{I_C R} = \frac{4}{\pi(1+\beta)} \exp\left(-3.5\pi^2 \frac{k_B T L}{\Phi_0^2}\right) \qquad (8)$$

We also investigated the dependance of the maximum voltage modulation on the asymmetry parameters of the DC SQUID (see Figs. 8 and 9). We have found that for M- and L-SQUIDs the influence of junction asymmetry on the voltage modulation is weaker than that for small inductance SQUIDs. For S SQUIDs there is appreciable scattering of ΔV_{max} versus γ and ρ.

B. Flux shift

As is known the asymmetry of the SQUID junctions results in a flux shift of the VFC under bias reversal. Here we determine the flux shift as the sum of the shifts of two VFCs, one for $I = +I_{max}$ and the other for $I =$

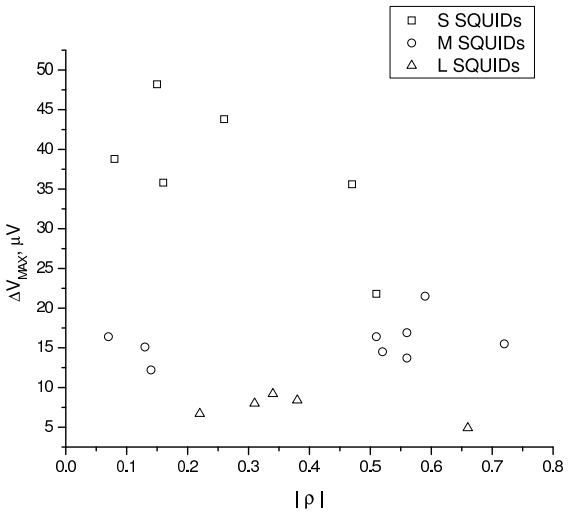

FIG. 9: The depth of the voltage modulation as a function of the resistance asymmetry ρ.

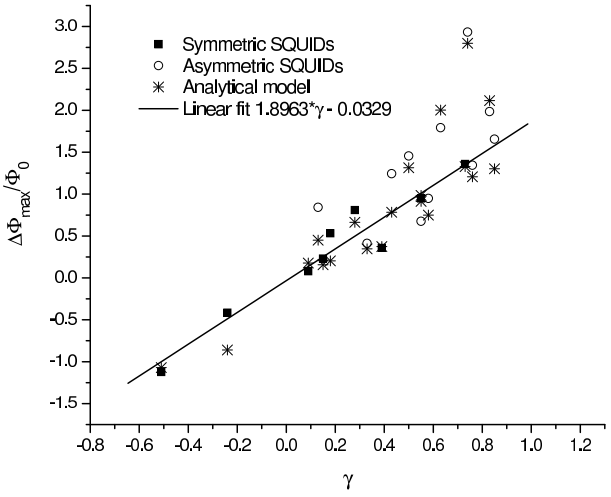

FIG. 10: The flux shift as a function of the current asymmetry γ. Geometrically symmetric SQUIDs ($\alpha_g = 0$) are shown by black boxes, SQUIDs with $\alpha_g \neq 0$ are shown by open circles. Theoretical points calculated from (7) are shown by stars.

$-I_{max}$, relative to the zero flux point ($I_{coil} = 0$ in Fig. 5). Here the subscript "max" means the bias current which provides maximum swing of the VFC. Since the VFC is Φ_0 periodic, the flux shift can be determined with an accuracy $2n\Phi_0$, where n is an integer. Thus the minimum uncertainty of the determination of the flux shift for asymmetrical SQUIDs is $2\Phi_0$.

In an ideal case when there is no parasitic trapped flux in the loop, both VFCs are shifted symmetrically by the same amount $\Delta\Phi_{sym}$ in opposite directions with respect to zero flux point. In this case the overall flux shift is calculated as a sum of both shifts, $\Delta\Phi = 2\Delta\Phi_{sym}$. However, in our cases the shift of two VFCs is not symmetric with respect to zero point (see Fig. 5). The reason for this is the parasitic flux Φ_p trapped in a loop. This flux does not change its sign under bias reversal, hence the flux shifts are as follows: $\Delta\Phi_- = \Delta\Phi_{sym} + \Phi_p$, $\Delta\Phi_+ = -\Delta\Phi_{sym} + \Phi_p$, where $\Delta\Phi_-$ is the flux shift for the VFC for reversed bias current ($I = -I_{max}$), and $\Delta\Phi_+$ is the same quantity for the unreversed VFC ($I = +I_{max}$). Thus, the parasitic flux disappears from the overall flux shift $\Delta\Phi = \Delta\Phi_- - \Delta\Phi_+ = 2\Delta\Phi_{sym}$. The application of this simple formula requires precise knowledge of the corresponding extremums of the VFCs shifted by a parasitic flux. In other words, we must know these two extremum points on both VFCs whose distance provides us with the overall flux shift. However, since VFC is Φ_0 periodic, it is not possible to definitely determine these two points. Therefore, a single valued determination of the flux shift requires some additional information.

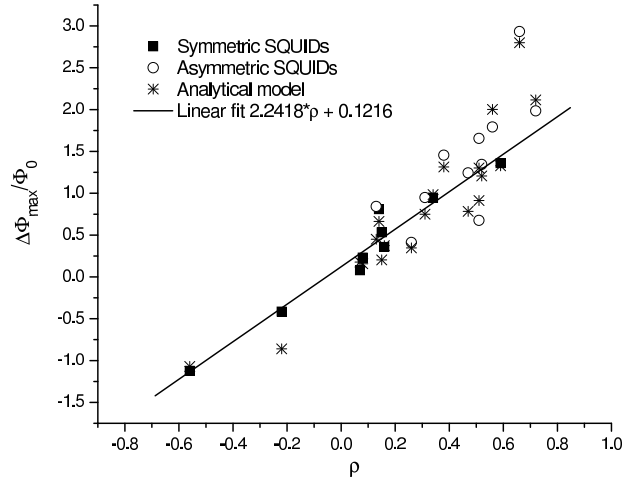

FIG. 11: The flux shift as a function of the resistance asymmetry ρ. Geometrically symmetric SQUIDs ($\alpha_g = 0$) are shown by black boxes, SQUIDs with $\alpha_g \neq 0$ are shown by open circles. Theoretical points calculated from (7) are shown by stars.

The procedure we used for the unique determination of the actual flux shift, $\Delta\Phi_{act}$ was performed in three steps. First, we measured the flux shift $\Delta\Phi_{meas}$ between the *nearest* extremum points of VFCs with respect to the zero flux point. Second, by using expression (7) we calculated for a given SQUID a theoretical value of the flux shift $\Delta\Phi_{theor}$. Finally, the actual flux shift $\Delta\Phi_{act}$ was determined by subtracting from (or adding to) $\Delta\Phi_{meas}$ the integer number of flux quanta $n\Phi_0$ ($n = 0, \pm1, \pm2, etc.$) which gave the flux shift nearest to the theoretical value $\Delta\Phi_{theor}$.

The illustration of our method is presented in Table IV. The values of actual flux shift from the last column of this table are given as $\Delta\Phi_{max}$ in the second column of Table II.

We want to stress here that in our method the theoretical estimations of the flux shift were used only as a guide

TABLE IV: Determination of actual flux shift. $\Delta\Phi_{meas}$ is the flux shift measured between nearest extremums of two VFCs, $\Delta\Phi_{theor}$ is the flux shift calculated from Eq. 7, and $\Delta\Phi_{act}$ is the actual flux shift corrected for parasitic flux.

SQUID# group	$\Delta\Phi_{meas}$ Φ_0	$\Delta\Phi_{theor}$ Φ_0, Eq.(7)	$\Delta\Phi_{act}$ Φ_0
1 S	0.357	0.374	0.357
2 S	1.532	0.203	1.532-1=0.532
3 S	1.675	0.913	1.675-1=0.675
4 S	1.23	0.157	1.23-1=0.23
5 S	0.412	0.347	0.412
6 S	1.243	0.784	1.243
7 M	1.36	1.328	1.36
8 M	0.079	0.177	0.079
9 M	0.656	1.302	0.656+1=1.656
10 M	-1.124	-1.07	-1.124
11 M	0.81	0.663	0.81
12 M	0.842	0.451	0.842
13 M	1.344	1.207	1.344
14 M	0.985	2.116	0.985+1=1.985
15 M	0.792	2.002	0.792+1=1.792
16 L	0.947	0.984	0.947
17 L	0.948	0.75	0.948
18 L	-0.415	-0.86	-0.415
19 L	0.455	1.315	0.455+1=1.455
20 L	0.934	2.8	0.934+2=2.934

for the determination of the actual flux shift caused by the predetermined asymmetry. This differs from many other papers on the subject (see, for example, Ref. 17) where theoretical expression (6) itself has been used for the determination of asymmetry parameters. In this latter case there are not any means which allow a unique discrimination between the unshifted curve and the curve shifted by a parasitic flux.

The dependance of experimental flux shift (second column in Table II) on current asymmetry γ and resistance asymmetry ρ is given in Figs. 10 and 11. Also we show on these graphs the theoretical points (star symbols) which were calculated from Eq. (7) by using the measured values of γ and ρ. As is seen from these graphs, the equation (7) is a good approximation for the measured flux shift. The experimental points for the flux shift can be approximated by least mean square fits which are as follows: $\Delta\Phi_{max}/\Phi_0 = 1.89\gamma - 0.03$ for Fig. 10 and $\Delta\Phi_{max}/\Phi_0 = 2.24\rho + 0.12$ for Fig. 11.

C. Transfer function

For every SQUID the transfer functions $V_\Phi^\pm$ were measured (see Table II) and their dependance on different SQUID parameters was investigated. The dependance of $V_\Phi^\pm$ on the loop inductance L is shown in Fig. 12. We also show on this plot the transfer function for a symmetric shape of the VFC by using the relation $V_\Phi = \pi\Delta V/\Phi_0$

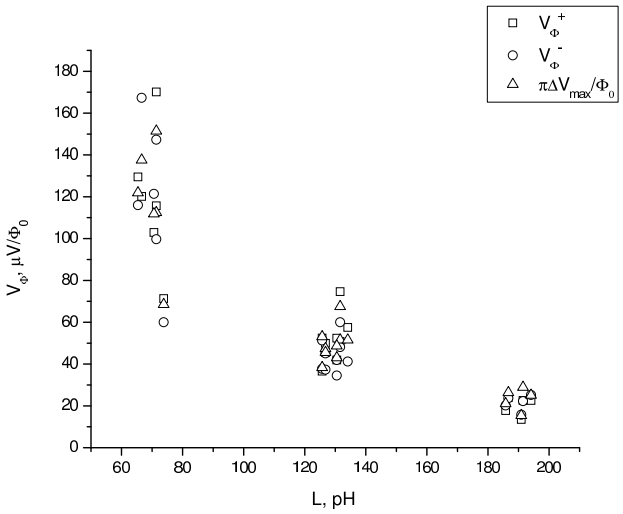

FIG. 12: Dependance of the transfer functions $V_\Phi^\pm$ on SQUID inductance.

with ΔV being taken from Table I. It is seen that, in general, the increase of inductance results in a decrease of both the transfer functions and the scattering for the transfer function values. The largest scattering is observed for S SQUIDs. Another conclusion is that as the SQUID inductance is increased the shape of VFC becomes more symmetric: the transfer function for symmetric shape becomes closer to the measured transfer functions $V_\Phi^\pm$. As a measure of the shape asymmetry of VFC we introduce the quantity $|V_\Phi^+ - V_\Phi^-|$ which is equal to zero for a symmetrical shape. The dependance of this quantity on SQUID inductance is shown in Fig. 13. From this figure it is clearly seen that the shape of VFC becomes more symmetric as the SQUID inductance becomes larger.

The dependance of the measured transfer functions $V_\Phi^\pm$ on β is shown in Fig. 14. Here one can see a nearly exponential decay of the transfer function with the increase of β.

The dependance of the normalized transfer functions $V_\Phi^\pm\Phi_0/RI_C$ on current asymmetry γ and resistance asymmetry ρ is shown in Figs. 15 and 16. As is seen from these figures, the L SQUIDs show a weak dependance on the parameters of asymmetry. It conforms with Fig. 13, where the VFCs for these SQUIDs have minimum distortion. However, for SQUIDs with small inductance (S SQUIDs) the dependance on asymmetry parameters is much stronger. It is worth noting that the γ and ρ dependances of $V_\Phi^\pm$ (see Figs. 15, 16) have indications of a peak for S SQUIDs near the value of 0.2. A similar behavior has been found for SQUIDs with $L \approx 20$ pH in Ref. 17 (see Fig. 6 therein).

We also compare the dependance of measured transfer functions V_Φ^+ on current asymmetry $\mid \alpha_J \mid$ for geometrically symmetric SQUIDs ($\alpha_g = 0$) with the corresponding expressions from Ref. 17 obtained from computer

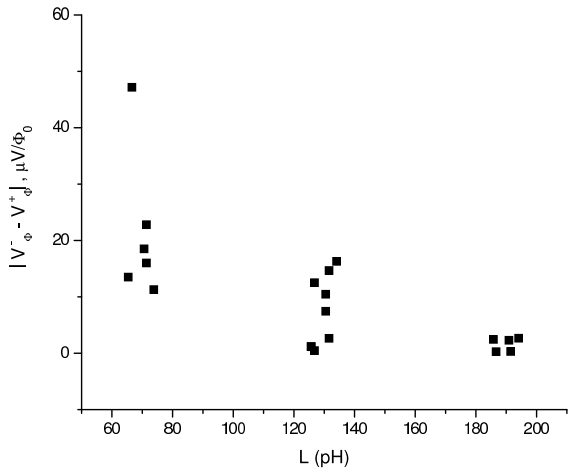

FIG. 13: The deviation of VFC shape from symmetrical form.

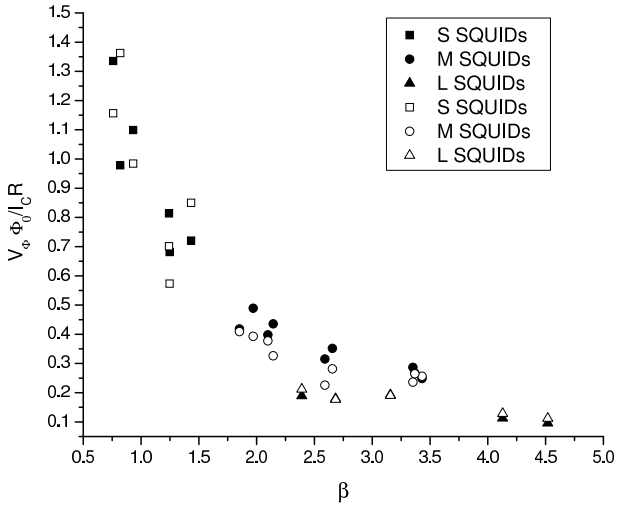

FIG. 14: Dependance of the transfer functions on β. Black symbols are for V_Φ^+, white symbols are for V_Φ^-.

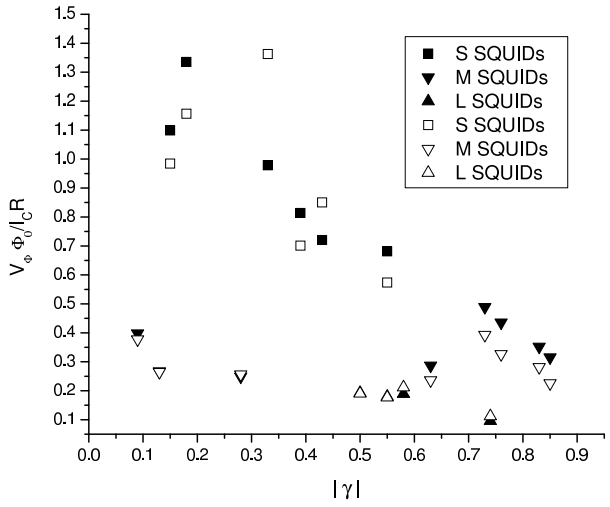

FIG. 15: Dependance of the transfer functions on current asymmetry γ. Black symbols are for V_Φ^+, white symbols are for V_Φ^-.

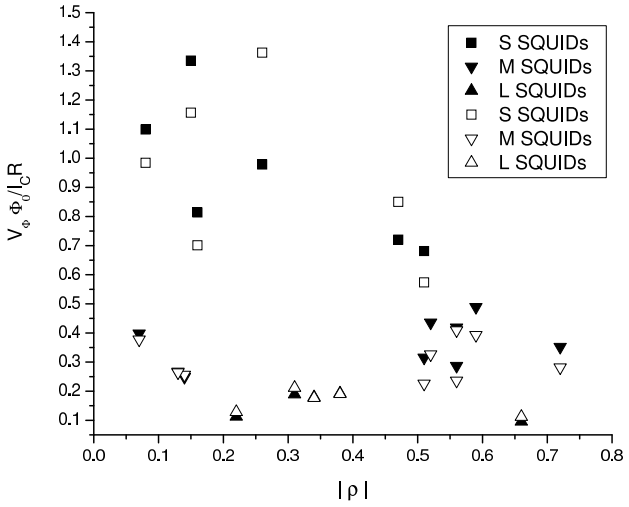

FIG. 16: Dependance of the transfer functions on resistance asymmetry ρ. Black symbols are for V_Φ^+, white symbols are for V_Φ^-.

simulations. The results are shown in Fig. 17. Again, the strongest deviation of experimental points from theoretical ones is observed for S SQUIDs (only SQUID #7 is an exception).

V. CONCLUSION

The main purpose of the study was the experimental investigation of the influence of the junction asymmetries on the SQUID output characteristics (depth of modulation, flux shift, transfer function). To this end we directly measured the current and resistance asymmetry of the junctions in every of 20 investigated SQUIDs. It turned out that the values of current and resistance asymmetry (α_j and α_ρ) were randomly distributed over a chip without noticeable correlation either with SQUID inductance or critical current. Even for geometrically symmetric SQUIDs (we had 9 such SQUIDs) there was a significant asymmetry in critical current and resistance. Nevertheless we achieved definite conclusions about the influence of the junction asymmetry on the SQUID output characteristics.

The dependance of the depth of modulation ΔV and the transfer functions $V_\Phi^\pm$ on the junction asymmetry is appreciable only for low inductance SQUIDs (see Figs. 8, 9, 15, 16). For large inductances this dependance is rather weak which is in accordance with a small distortion of the shape of VFC for these SQUIDs (see Fig.

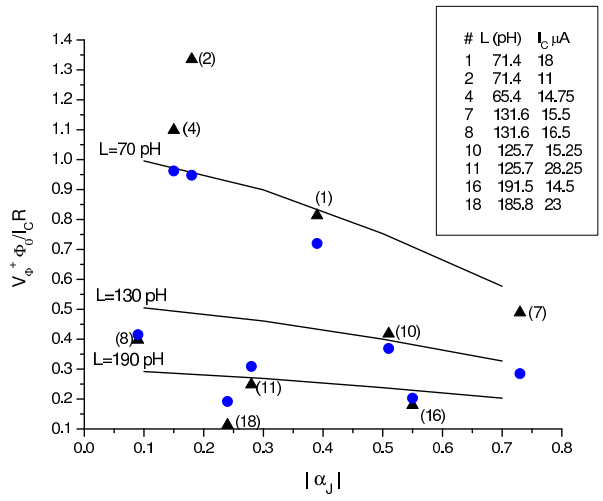

FIG. 17: Color online. The transfer function V_Φ^+ for geometrically symmetric SQUIDs ($\alpha_g = 0$). Black triangles with SQUID # are experimental points; blue circles are corresponding values calculated by using Eqs. 6 for intrinsic asymmetry from Ref.17. Solid lines show a guide dependance for three different inductances calculated from the same equations for $I_C = 15\mu A$. The insert shows the values of inductance and critical current for SQUIDs with $\alpha_g = 0$ taken from Table I.

13). Therefore, we may conclude that, in general, both the voltage modulation and the transfer function are not very sensitive to the junctions asymmetry. However, for SQUIDs with a relatively small inductance $L < 70$ pH the dependance on asymmetry is more significant, the shape of VFC is more distorted and the transfer functions are well above the corresponding values for large inductance SQUIDs.

As was expected, the flux shift of the VFC is more sensitive to the junction asymmetry than the depth of modulation or transfer functions. The dependance of the flux shift on γ and ρ is approximately linear and it is well described by the analytical model (Figs. 10, 11).

The results obtained in the paper are important for the implementation in the sensitive instruments based on high T_C SQUID arrays and gratings.

Acknowledgment

The authors are indebted to V. Zakosarenko for helpful discussions related to the measurements, and to M. Sondermann and S. Giessler for the preparation of SQUID chips for the measurements. Ya. S. G. thanks J. T. Jeng for useful comments and for providing the manuscript of his contribution to ASC'08 prior its publication. I. L. N. acknowledges the hospitality of the Institute of Photonic Technology, Jena, Germany, where the experimental part of the work has been performed. The work was partly supported by DAAD and Ministry of Education and Science of Russian Federation (Programm "Michail Lomonosov", Grant # 9686).

[1] D. Koelle, R. Kleiner, F. Ludwig, E. Dankster, John Clarke, Rev. Mod. Phys. 71, 631 (1999).
[2] F. Ludwig, E. Dantsker, R. Kleiner, D. Koelle, John Clarke, S. Knappe, D. Drung, H. Koch, Neil McN. Alford and Tim W. Button, Appl. Phys. Lett. 66, 1418 (1995).
[3] M. I. Faley, U. Poppe, K. Urban, D. N. Paulson, T. N. Starr, and R. L. Fagaly, IEEE Trans. Appl. Supercond. 11, 1383 (2001).
[4] V. Schultze, V. Zakosarenko, R. Usselsteijn, J. Ramos, H. G. Meyer, IEEE Trans. Appl. Supercond. 9, 3279 (1999).
[5] M. Matsuda, K. Nakamura, H. Mikami, and S. Kuriki, IEEE Trans. Appl. Supercond. 15, 817 (2005).
[6] J. H. Miller, G. H. Gunaratne, Z. Zou; M. F. Davis; H. R. Rampersad, N.-Q. Fan, and J. C. Wolfe, Proc. SPIE, 2160, 41 (1994).
[7] V. Schultze, R. IJsselsteijn, H.G. Meyer, J. Oppenlander, C.Haussler, N. Schopohl, IEEE Trans. Appl. Supercond. 13, 775 2003.
[8] R. Gerdemann, K. D. Husemann, R. Gross, L. Alff, A. Beck, B. Elia, W. Reuter, and M. Seigel, J. Appl. Phys. 76, 8005 (1994).
[9] P.Shadrin, C. L. Jia and Y. Divin, Physica C 372-376, 80 (2002).
[10] P. Shadrin, C. L. Jia and Y. Divin, IEEE Trans. Appl. Supercond. 13, 603 (2003). [14]
[11] J.T. Jeng and Y.C. Lin, Chin. J. Phys. 45, 175 (2007).
[12] J.T. Jeng, C. C. Lu, C. C. Wang, C. Y. Wu, Appl. Supercond. Conf. 17-22 Aug., 2008, Chicago, USA.
[13] J. Beyer, D. Drung, F. Ludwig, T. Minotani, K. Enpuku, Appl. Phys. Lett. 72, 203 (1998).
[14] K. Park, S.-G. Lee, H.C. Kwon, Y.K. Park, J.-C. Park, IEEE Trans. Appl. Supercond. 5, 3119 (1995).
[15] Q. Jia, F. Yan, C. Mombourquette, D. Reagor, Appl. Phys. Lett. 72, 3068 (1998).
[16] R. Kleiner, D. Koelle, F. Ludwig, E. Dantsker, A.H. Miklich and John Clarke, J. Appl.Phys. 79, 1129 (1996).
[17] J. Mueller, S. Weiss, R. Gross, R. Kleiner, D. Koelle, IEEE Trans. Appl. Supercond. 11, 912 (2001).
[18] G. Testa, E. Sarnelli, S. Pagano, C.R. Calidonna and M. Mango Furnari, J.Appl.Phys. 89, 5145 (2001).
[19] G. Testa, C. Granata, C. Calidonna, C. Di Russo, M. Mango Furnari, S. Pagano, M. Russo, E. Sarnelli, Physica C 368, 232 (2002).
[20] Ya. S. Greenberg, Physica C 383 (2003) 354.
[21] R. Gross, L. Alff, A. Beck, O. M. Froehlich, D. Koelle, A. Marx, IEEE Trans. Appl. Supercond. **7**, 2929 (1997).
[22] J. Ramos, M. Seitz, G.M. Daalmans, D. Uhl, Z. Ivanov, T. Claeson, Physica C **220**, 50 (1994).
[23] S. Weiss, D. Koelle, J. Muller, R. Gross, K. Barthel, Europhys. Lett. **51**, 499 (2000).
[24] C.D. Tesche and J. Clarke, J.Low.Temp.Phys. 29, 301 (1977).
[25] R. IJsselsteijn, H. Elsner, W. Morgenroth, V. Schultze, and H.-G. Meyer, IEEE Trans. Appl. Supercond. **9**, 3498

(1999).
[26] R. IJsselsteijn, V. Schultze, and H.-G. Meyer, IEEE Trans. Appl. Supercond. **17**, 734 (2007).
[27] G. Hildebrandt and F.H. Uhlmann, IEEE Trans. On Magnetics **11**, 690 (1996).
[28] V. Ambegaokar and B. I. Halperin, Phys. Rev. Lett. **22**, 1364 (1969).
[29] K.Enpuku, G. Tokita, T. Maruo, and T. Minotani, J. Appl. Phys. 78, 3498 (1995).